ARMY RESEARCH LABORATORY

Structural Degradation of a Tank Cannon Due to Hole Damage

by Larry Burton

ARL-TR-1796

September 1998

Approved for public release; distribution is unlimited.

Abstract

An analysis was undertaken to determine the deleterious effects upon the M256 tank cannon's structural integrity if it were perforated. The analytical study looked at holes ranging in diameter from 1.5 in (3.8 cm) to 4.0 in (10 cm). Two perforation scenarios were modeled: one having a centered through hole and the other with a single hole centered on the cannon's wall. Finite element analysis runs were made to determine the extent of the plastic deformation that resulted from the introduction of the hole. Two locations along the barrel's length were considered: one near the muzzle end and the other at the tube's midsection. The muzzle end exhibited a greater depth of plastic stress with nearly one-third of the gun tube wall going into the plastic regime for the largest hole sizes.

Table of Contents

INTENTIONALLY LEFT BLANK.

List of Figures

INTENTIONALLY LEFT BLANK.

List of Tables

INTENTIONALLY LEFT BLANK.

1. Introduction

Tank cannons serve as a containment structure for high-pressure propellant gases that undergo expansion resulting in acceleration of a projectile down-bore. At present, the principal means of defeating a main battle tank is via penetration of its frontal armor. It has been suggested that an alternate means of eliminating an enemy tank as a battlefield threat is to attack its cannon and render it inoperable. While the feasibility of hitting a tank's cannon, with a smaller presented area, may be debated, a technical assessment was required to determine the magnitude of structural damage needed to disable the gun barrel. This report details the analytical investigation made to ascertain the structural degradation of a tank's main cannon when it has been penetrated and damaged.

2. Procedure

Finite-element analysis (FEA) techniques were used to assess the structural integrity of a damaged gun tube. The damage was assumed to be in the form of a hole pierced through the barrel wall. The mechanism for producing the hole was not of importance for the analysis. The modeling effort assumed circular holes perpendicular to and centered about the gun tube's centerline.

Tank barrels are designed with a taper to correspond to the reduction in pressure experienced by the gun tube along its length. The exterior profile of the gun barrel is shown in Figure 1 and a plot of peak in-bore pressure vs. axial position is given in Figure 2. The size of the barrel made it difficult to create an FEA model of the entire barrel with sufficient grid refinement to capture the effects produced by a hole along the barrel length. Therefore, the approach taken was to model two different 5-in (12.7 cm) sections of the gun tube. One section modeled the barrel's muzzle end, while the other section chosen was located at approximately the center of the barrel's length. These regions are denoted on Figure 1, with the axial location and outside barrel diameter listed in Table 1. For the purpose of this analysis, there was no pressure gradient over the 5-in (12.7 cm) section lengths assumed. Instead, an average pressure for each region was uniformly applied. A value of 9,000 psi (62 MPa) was used for the muzzle region, and 22,535 psi (155 MPa) for the midsection.

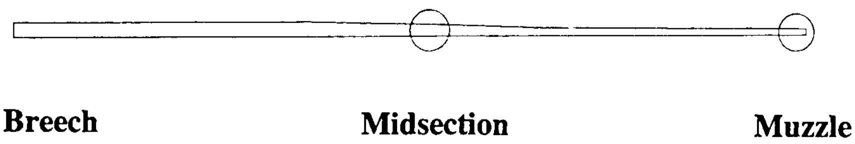

Figure 1. M256 Tank Cannon Exterior Profile.

Table 1. Axial Location and Outside Barrel Diameter

Location	Distance From Breech (in [cm])	Outside Diameter at Section End Nearest Breech (in [cm])	Outside Diameter at Section End Furthest From Breech (in [cm])
Midsection	107.89 [274.04]	7.82 [19.9]	7.71 [19.6]
Muzzle	208.7 [530.1]	6.33 [16.1]	6.30 [16.0]

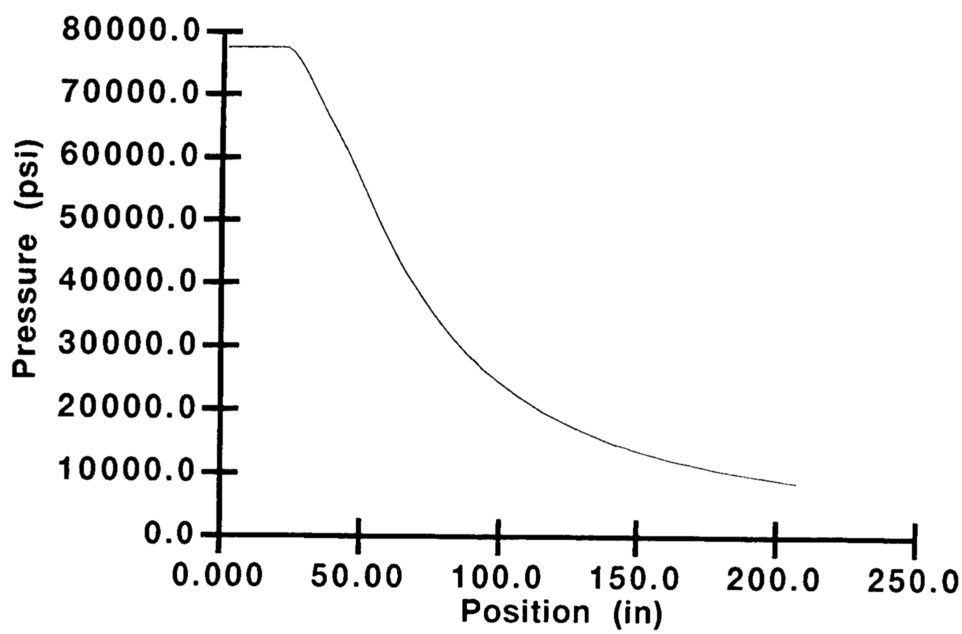

Figure 2. Pressure-Time Curve for the M256 Cannon.

The purpose of the analysis was to assess structural integrity of a damaged tank cannon. For the FEA modeling, this damage took the form of a hole in one of the sections of interest made by a long-rod penetrator, for example. Two different scenarios were investigated: one being a hole that pierced through just one wall of the barrel and the second being one that passed completely through the gun tube structure and resulted in a through-hole, that is, identical holes 180° apart. Hole size was varied from 1.5 to 4.0 in (3.8 to 10.2 cm), with analysis runs made for each 0.5-in (1.3 cm) increment.

The ANSYS FEA code (Swanson 1992) was used with 8-node brick elements employed to model the 120-mm M256 tank cannon. Material characteristics provided for the gun steel included an elastic modulus of 29×10^6 psi (200 GPa) and a multilinear kinematic-hardening plasticity model that is shown in Figure 3 (O'Hara 1996). Symmetry was used to reduce the size of the models and computations, and thus allow for finer meshing of the region surrounding the hole. The through-hole cases required that only one-quarter of the tube be modeled, while the cases of a hole through a single sidewall necessitated one-half of the structure be modeled.

The models were constructed using Boolean operations provided in the ANSYS finite-element code. Initially, the quarter-symmetry model was comprised of four volumes that were formed by making a vertical slice through the length of the 5-in (12.7 cm) section and a longitudinal cut along the length of the 90° arc. Figure 4 shows such a group of volumes with one-quarter of a hole through the top of the model. The arrangement of volumes used for the meshing varied between models. For example, the 2.5-in-diameter (6.4 cm) case had the vertical cutting plane positioned at midlength, with the cut through the length made at 45° around the arc. Holes larger than this required that the geometry model be broken down into more volumes to avoid poor element shapes. Figure 5 shows an example of the volumes used to build the model for the 3.5-in (8.9 cm) hole analysis. A vertical cut was made 2 in (5 cm) from the y-axis with another slice taken 30° from the axis labeled "wy" in the figure. The midregion model was done similar to the muzzle end with additional volumes used to model the underside of the barrel.

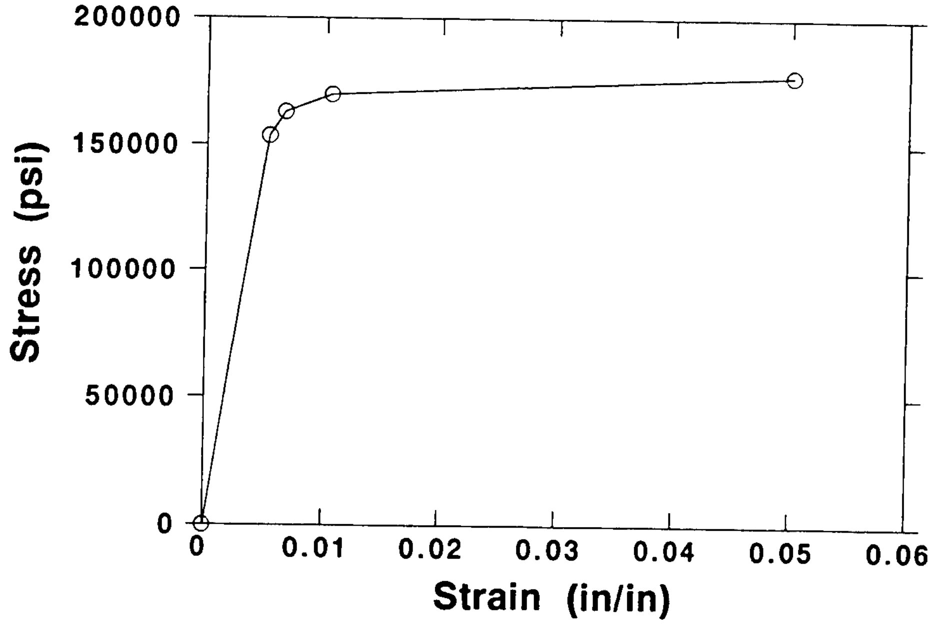

Figure 3. Plasticity Model for M256 Gun Steel.

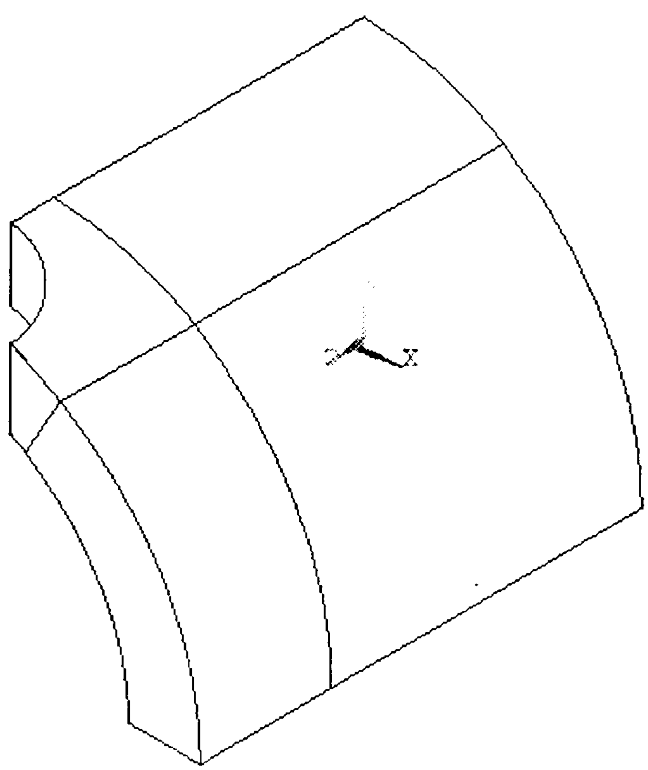

Figure 4. Initial Volume Modeling for Quarter-Symmetry Model.

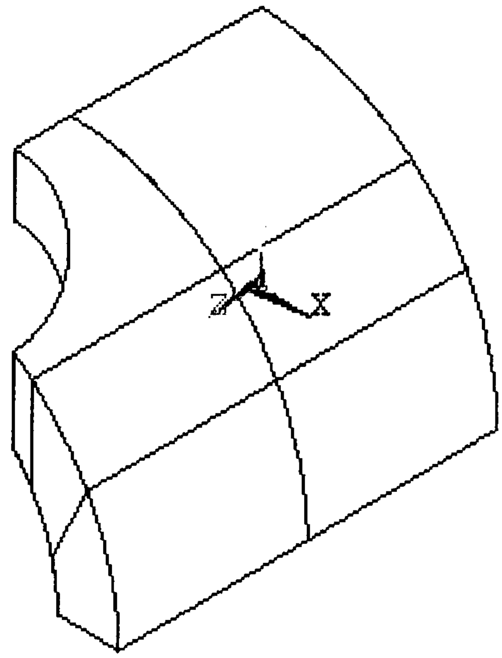

Figure 5. Volume Modeling for Larger Hole Sizes.

Initially, the muzzle end of the gun barrel was modeled and analyzed without any holes to determine the model size that could be handled by the HP720 computer system and to verify the symmetry boundary conditions. Figure 6 shows the results of this quarter-barrel model, which imposed symmetry boundary conditions on both planes along the length (z-direction) of the 5-in (12.7 cm) section. A zero displacement condition was placed on the rear-cut face of the tube. The muzzle end or front face of the model was unconstrained. For the midsection case, a zero displacement condition was imposed on the front face. The view in Figure 6 is from the breech end of the cannon looking out toward the muzzle. The maximum equivalent stress calculated for the quarter-symmetry model was 37,058 psi (256 MPa) on the wall during the launch cycle, which is identical to the analytical calculation for a simple pressure vessel, thus verifying the correctness of the boundary conditions.

3. Through-Hole Results

The through-hole analysis began with a barrel having a 1.5-in (3.8 cm) hole near the muzzle. The region around the hole was modeled with 10 elements over a length extending 0.75 in (1.9 cm)

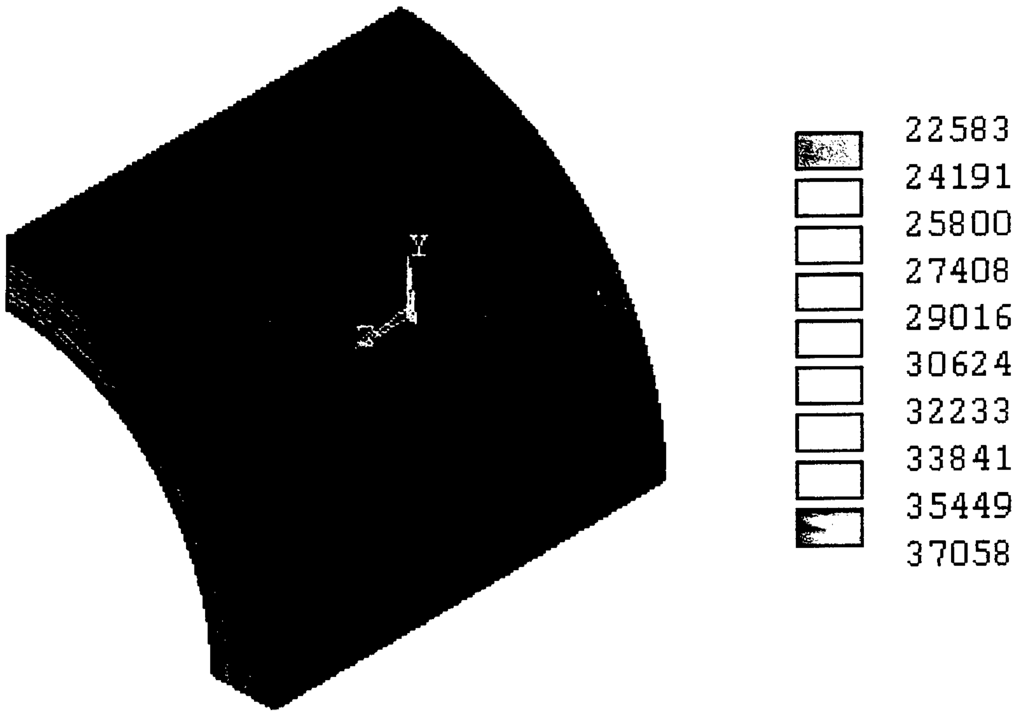

Figure 6. Quarter-Symmetry Model of M256 at the Barrel Midsection.

from the hole's edge. Nodes were spaced such that the element farthest from the hole was five times the size of the element adjacent to the hole's edge. The maximum equivalent stress was found to be approximately 133,000 psi (917 MPa), well below the steel's yield point and, therefore, this size hole does not threaten the integrity of the gun tube. To ensure that a convergent solution had been achieved, two more element grids with increased element densities near the hole were constructed for this barrel geometry. The second grid pattern increased the ratio of the size of the furthest element from the hole (over the 0.75-in [1.9 cm] length) to that nearest from 5:1 to 10:1. This resulted in more elements closer to the area of high stress being found in the original analysis. A blown-up view of the elements in this region is depicted in Figure 7. The resulting maximum stress for this grid pattern was equivalent to that of the original model.

The first two models both had 10 elements of uniform width distributed through the thickness of the barrel. Like the second model, the third grid examined in the convergence analysis employed a 10:1 ratio for the element size along the axial and circumferential edges nearest the hole. However, the through-the-thickness distribution of elements was changed from equal sizing to a 10:1 size ratio for the elements nearest the outside wall to those closest to the bore, as shown in Figure 7. The

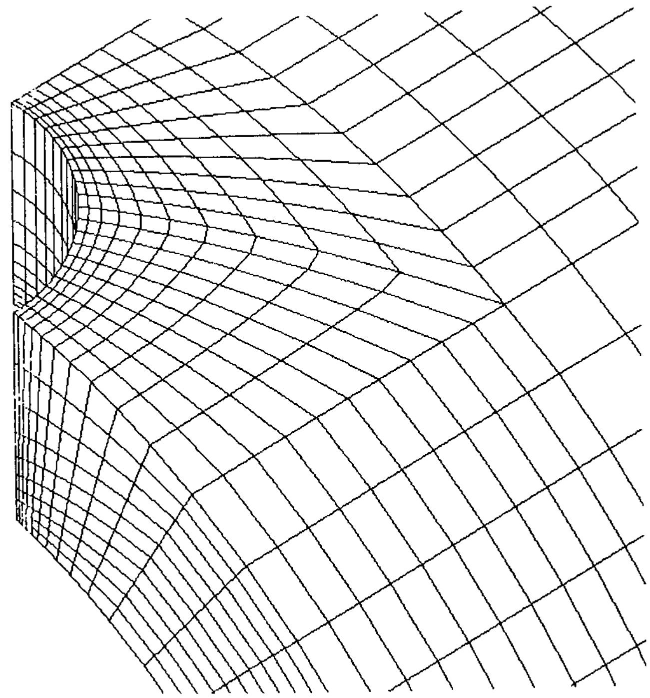

Figure 7. Exploded View of 1.5-in (3.8 cm) Hole at the Muzzle.

increased element density near the bore corresponded to the area of highest stress in the first two analyses. This grid scheme produced a maximum stress equivalent to those found with the first two models that uniformly spaced elements through the wall thickness. To ensure convergence, the vertical displacements of the nodes along the axial edge of the bore surface were plotted for each of the grid schemes and are shown in Figure 8. The displacements for the three cases are plotted against their position along the barrel, where zero represents the muzzle. The only discernible difference between the three results is in the region nearest the hole. Figure 9 plots an exploded view of this region, where the differences are seen to be on the order of a 10^{-5}-in (2.5×10^{-5} cm) magnitude, showing that the solutions are convergent.

The 10:1 element-size ratio along the axial length of the hole and the equal element size through the barrel thickness (as used in the second grid geometry) were adopted and maintained for all other analysis runs. Since this distribution of nodes and elements had resulted in a convergent solution for the 1.5-in (3.8 cm) case, it was assumed to do so for the larger hole sizes. Thus, convergent studies for the larger holes were not done.

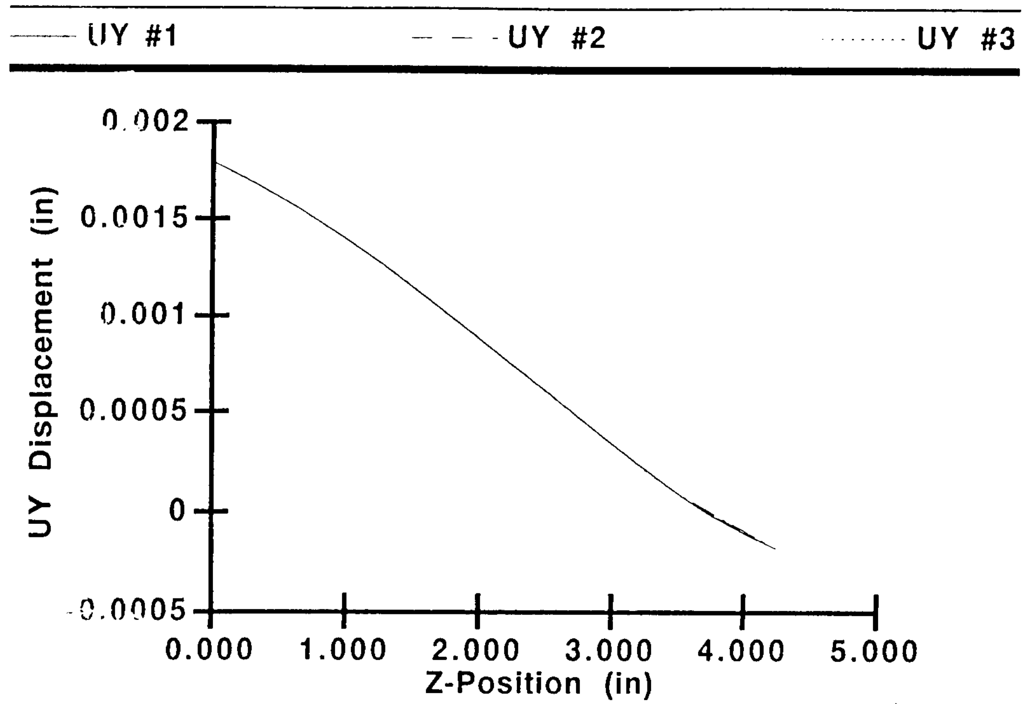

Figure 8. Nodal Displacement Plot for Different Element Grids.

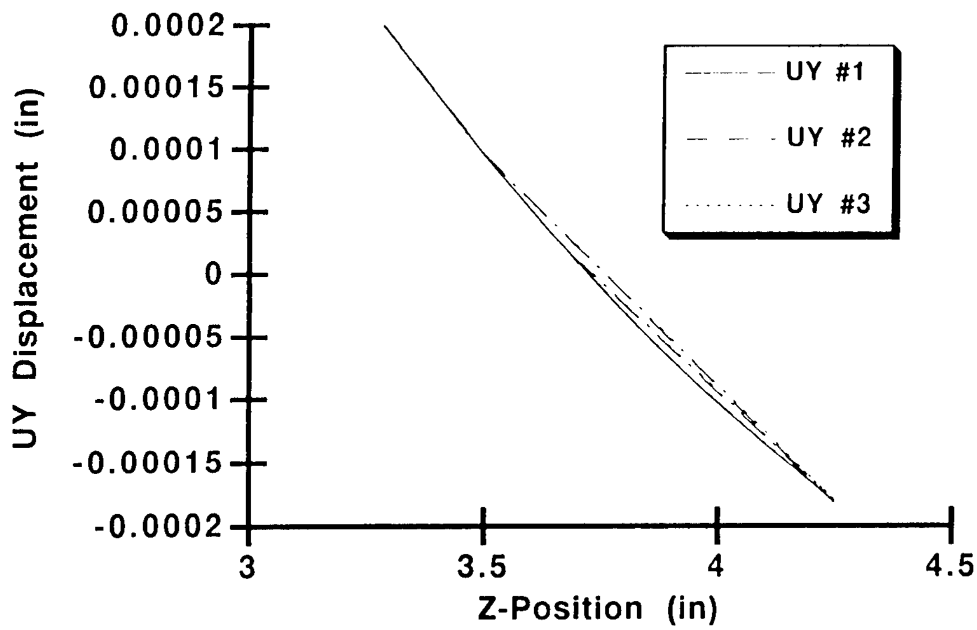

Figure 9. Exploded View of Nodal Displacement Plot.

The hole size was then increased to 2 in (5 cm), with the results showing a very minute region around the hole exceeding the yield stress of the gun steel. The resulting plastic deformation was infinitesimal and not sufficient to threaten the integrity of the gun tube during projectile launch.

The 2.5-in (6.4 cm) hole-diameter analysis found the first appreciable amount of plastic stress in the region around the hole. A plot of the equivalent stress for the entire model is given in Figure 10. An expanded view of the highly stressed edge of the hole is also provided, with the stress contours adjusted so that all colors other than dark blue represent stress values exceeding yield. It is seen that the plastic stress extends 12% through the thickness, which is 0.8 in (2.0 cm) at this edge. This percentage depth of plasticly stressed material was used as a barometer for the damage to the gun tube resulting from a hole to allow for comparison with other hole sizes.

Subsequent runs were made in 0.5-in (1.3 cm) increments for holes up to 4-in (10 cm) in diameter at both the barrel's muzzle end and midsection. Table 2 lists the maximum plastic stress experienced at the hole's edge, as well as the percentage depth into the thickness that the plastic region extends. It is apparent from Table 2 that the muzzle end undergoes more plastic deformation than the barrel's midsection for a given hole size. Figures 11–14 show plots with corresponding stress values for each directional stress component for the case of the 2.5-in (6.4 cm) hole at the muzzle.

Notice that the stress component in the x-direction, σ_x (Figure 12), is the primary contributor to the maximum equivalent stress values seen in Figure 11. The x-direction is perpendicular to the plane of the hole's axis and the gun-bore centerline. The elevated stress in this direction results from the internal pressure applied to the gun bore, which acts to tear the hole open along the length of the barrel. At the barrel's midsection, the undamaged length in front of the hole acts to constrain the transverse load resulting from the hole. The muzzle end of the barrel lacks such a constraint.

Further examination of Table 2 shows that no appreciable plastic deformation occurs until a 2.5-in-diameter (6.4 cm) hole is achieved. The 4-in (10 cm) hole results in the most penetrating depth of plastic stress, and this is still less than one-third the way through the thickness. While there is deformation in this region, it turns out to be the result of bending of the barrel around the hole.

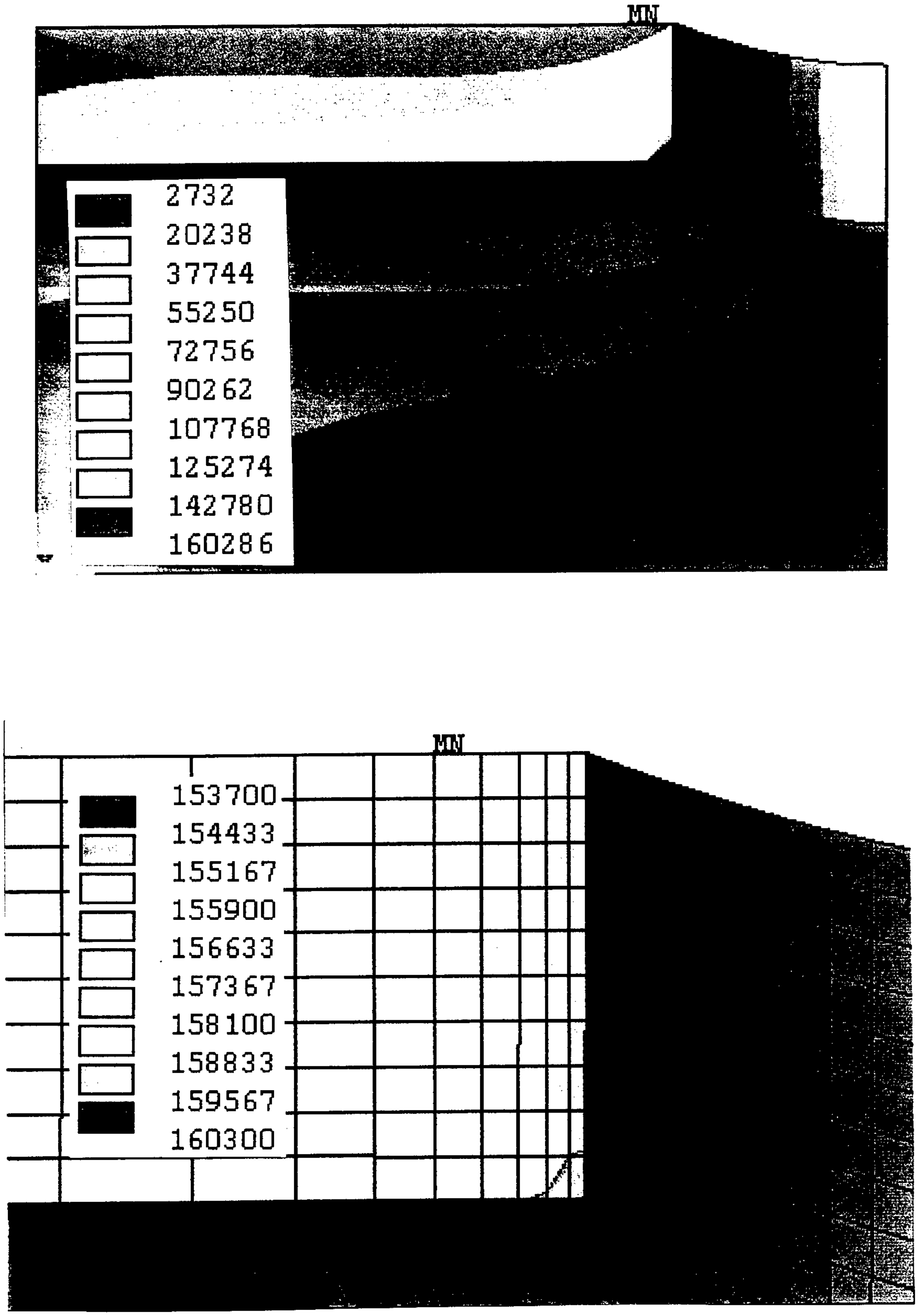

Figure 10. Equivalent Stress Plot of 2.5-in (6.4 cm) Hole at the Muzzle.

Table 2. Through-Hole Analysis Data

Location	Hole Diameter (in [cm])	Maximum Stress (kpsi [MPa])	Depth of Plastic Stress (%)
Muzzle	1.5 [3.8]	133.6 [921]	—
Muzzle	2.0 [5.1]	155.3 [1,071]	1
Muzzle	2.5 [6.4]	160.3 [1,105]	12
Muzzle	3.0 [7.6]	164.1 [1,131]	22
Muzzle	3.5 [8.9]	165.9 [1,144]	30
Muzzle	4.0 [10.2]	167.6 [1,156]	32
Midbarrel	1.5 [3.8]	152.6 [1,052]	—
Midbarrel	2.0 [5.1]	158.7 [1,094]	4
Midbarrel	2.5 [6.4]	159.3 [1,098]	11
Midbarrel	3.0 [7.6]	162.2 [1,118]	18
Midbarrel	3.5 [8.9]	163.4 [1,127]	20
Midbarrel	4.0 [10.2]	163.3 [1,126]	12

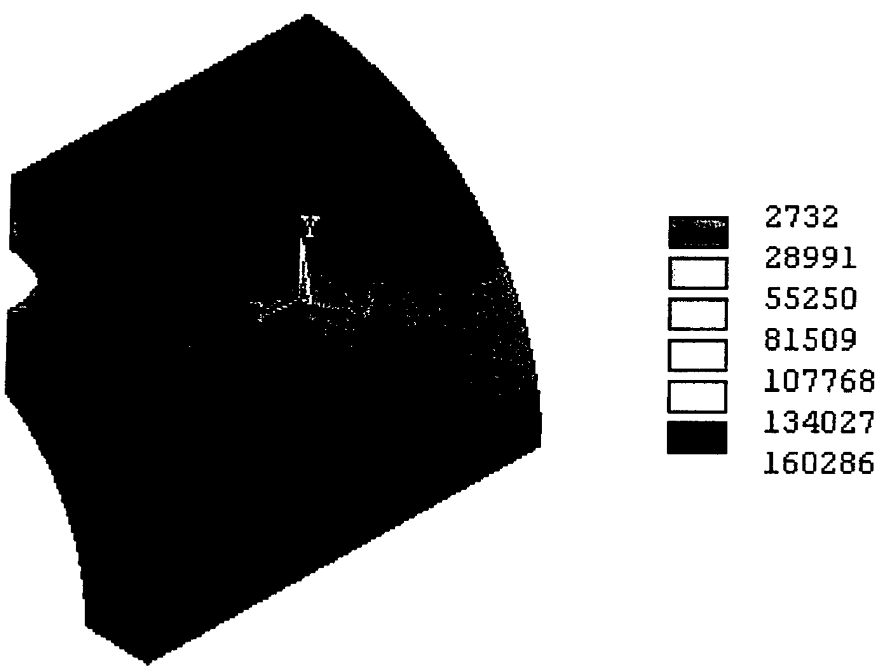

Fgure 11. Von Mises Effective Stress for 2.5-in (6.4 cm) Hole at the Muzzle.

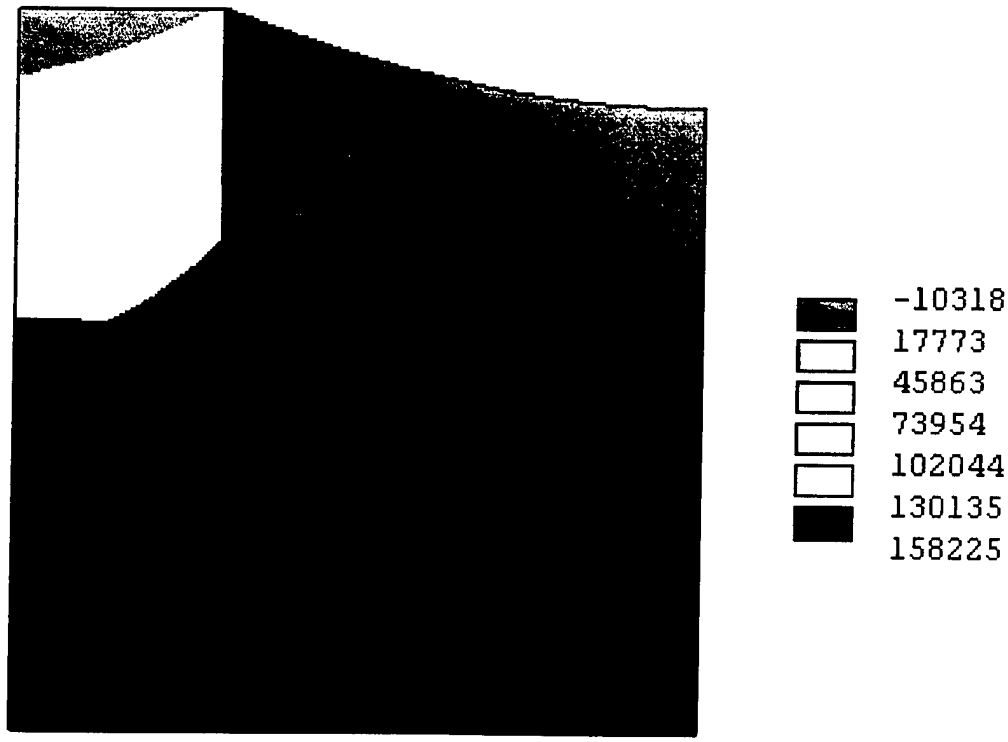

Figure 12. Directional Stress Component, σ_x, for 2.5-in (6.4 cm) Hole at the Muzzle.

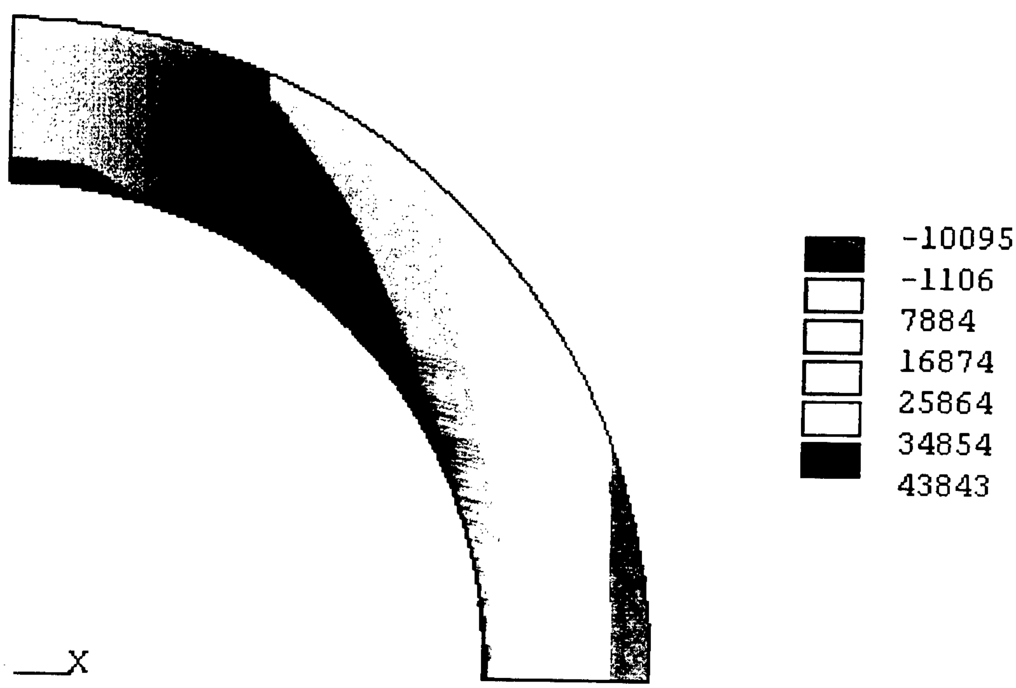

Figure 13. Directional Stress Component, σ_y, for 2.5-in (6.4 cm) Hole at the Muzzle.

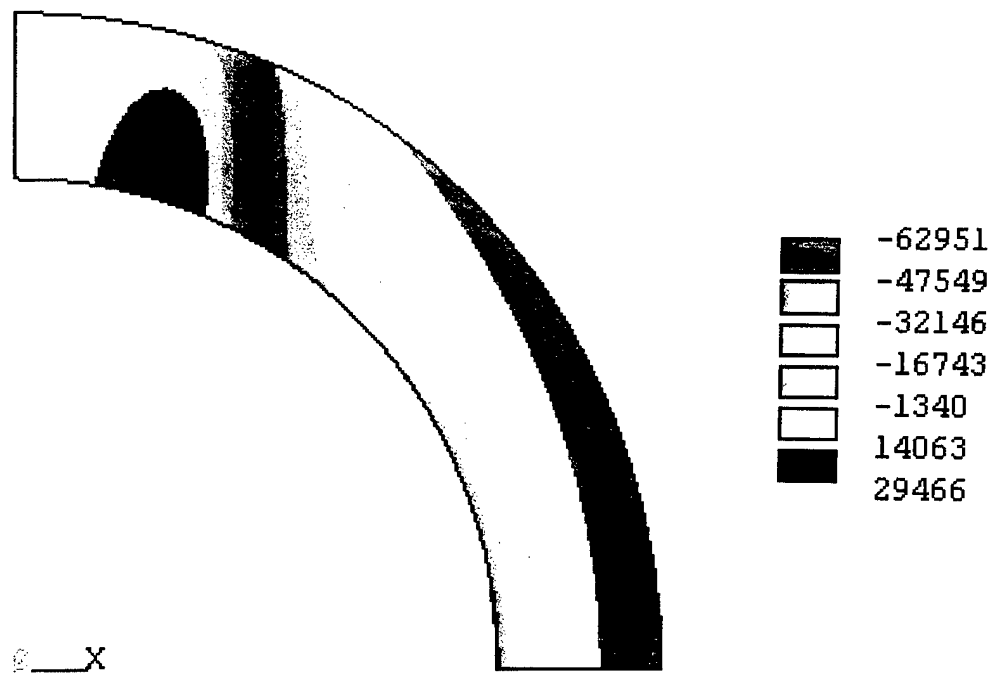

Figure 14. Directional Stress Component, σ_z, for 2.5-in (6.4 cm) Hole at the Muzzle.

An examination of the radial displacement of the nodes near the hole shows they actually move inward, despite the internal pressure, to decrease the bore radius by approximately 0.030 in (0.076 cm). This small deformation will not interfere with the round during launch.

4. Single-Hole Results

Since the muzzle end experienced the more extreme stress intensities of the two areas investigated for the through-hole analysis, it was decided to focus on this region for the single-hole investigation. Again, hole size was varied from 1.5- to 4.0-in (3.8 to 10 cm) diameters. The model geometry incorporated half of the gun tube structure as shown in Figure 15. Symmetry boundary conditions were used along the length of the muzzle section perpendicular to the plane, which slices the structure. A zero displacement was along the back face of the model, similar to what was done for the through-hole analysis. A final boundary constraint was required in the vertical y-direction to prevent rigid-body motion of the model. A single constraint was placed on the outer edge of the muzzle face and is located at the lower left corner of the model, as positioned in Figure 15. Imposing such a constraint resulted in a localized stress concentration. However, the location of the

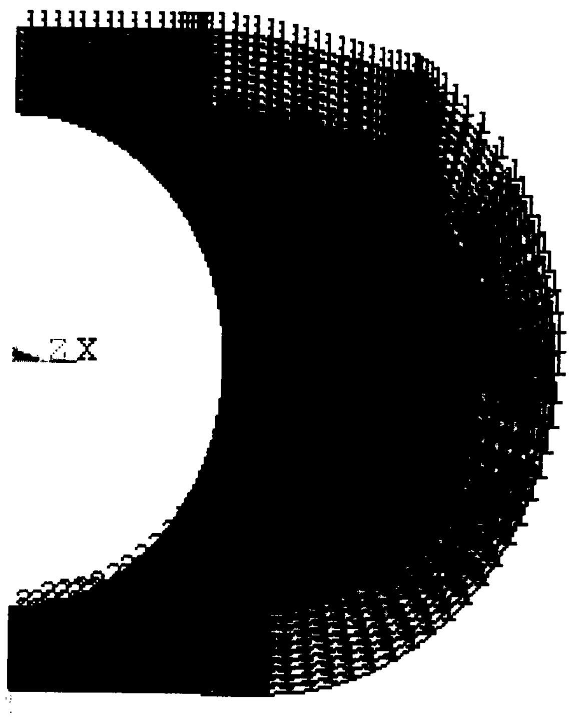

Figure 15. Single-Hole Model of Barrel's Muzzle End.

constraint was sufficiently far enough from the hole region that it did not influence the area of interest around the hole. In order to get convergent solutions, the single-hole cannon models used elastic material properties for the elements near the y-constraint (shown as red elements) and the plastic material data properties for the rest of the geometry (shown as blue elements).

Table 3 shows the compilation of the maximum stresses and percentage depth of plastic stress for the various hole sizes. Comparing these results with those for the muzzle end in Table 2, it is apparent that a single-hole analysis results in less severe loading of the barrel than a through-hole of comparable size.

5. Conclusion

This study was undertaken to determine if a gun tube could be rendered incapable of firing by piercing it with a hole. Both through holes and single holes were investigated, with hole size varied

Table 3. Single-Hole Analysis Data

Location	Hole Diameter (in [cm])	Maximum Stress (kpsi [MPa])	Depth of Plastic Stress (%)
Muzzle	2.0 [5.1]	148.0 [1,020]	—
Muzzle	2.5 [6.4]	158.5 [1,093]	6
Muzzle	3.0 [7.6]	161.0 [1,110]	12
Muzzle	3.5 [8.9]	164.4 [1,134]	20
Muzzle	4.0 [10.2]	164.9 [1,137]	21

up to 4 in (10 cm). The analysis showed that a through hole resulted in more deleterious effects to the gun tube than a single hole. The resulting analysis showed that a minimum hole diameter of 2.5 in (6.4 cm) is required to achieve any appreciable plastic deformation. Even larger hole sizes that produced greater deformations would not likely be sufficient to catastrophically fail the gun tube upon firing. However, this does preclude the possibility of an in-bore projectile failure. The design of the 120-mm M829 projectile is such that the obturator has a trailing overhanging length of 1.5 in (3.8 cm) that is subjected to the same pressure load as the gun tube. When the obturator passes over a large hole, it is unsupported against the pressure load and could fail. At the very least, the holes will result in a loss in muzzle velocity from that typically achieved, as found by Baer and Ruth (1981).

INTENTIONALLY LEFT BLANK.

6. References

Baer, Paul G., and Carl R. Ruth. "Interior Ballistics of Damaged Gun Tubes." BRL-MR-03071, U.S. Army Ballistic Research Laboratory, Aberdeen Proving Ground, MD, January 1981.

O'Hara, Glenn P. Private communication. U.S. Army Benet Laboratories, Watervliet Arsenal, NY, 3 June 1996.

Swanson Analysis Systems, Inc. "ANSYS User's Manual for Revision 5.0." Houston, PA, December 1992.

INTENTIONALLY LEFT BLANK.

NO. OF COPIES	ORGANIZATION
2	DEFENSE TECHNICAL INFORMATION CENTER DTIC DDA 8725 JOHN J KINGMAN RD STE 0944 FT BELVOIR VA 22060-6218
1	HQDA DAMO FDQ DENNIS SCHMIDT 400 ARMY PENTAGON WASHINGTON DC 20310-0460
1	OSD OUSD(A&T)/ODDDR&E(R) R J TREW THE PENTAGON WASHINGTON DC 20301-7100
1	CECOM SP & TRRSTRL COMMCTN DIV AMSEL RD ST MC M H SOICHER FT MONMOUTH NJ 07703-5203
1	PRIN DPTY FOR TCHNLGY HQ US ARMY MATCOM AMCDCG T M FISETTE 5001 EISENHOWER AVE ALEXANDRIA VA 22333-0001
1	DPTY CG FOR RDE HQ US ARMY MATCOM AMCRD MG BEAUCHAMP 5001 EISENHOWER AVE ALEXANDRIA VA 22333-0001
1	INST FOR ADVNCD TCHNLGY THE UNIV OF TEXAS AT AUSTIN PO BOX 202797 AUSTIN TX 78720-2797
1	GPS JOINT PROG OFC DIR COL J CLAY 2435 VELA WAY STE 1613 LOS ANGELES AFB CA 90245-5500

NO. OF COPIES	ORGANIZATION
1	DARPA B KASPAR 3701 N FAIRFAX DR ARLINGTON VA 22203-1714
1	NAVAL SURFACE WARFARE CTR CODE B07 J PENNELLA 17320 DAHLGREN RD BLDG 1470 RM 1101 DAHLGREN VA 22448-5100
1	US MILITARY ACADEMY MATH SCI CTR OF EXCELLENCE DEPT OF MATHEMATICAL SCI MDN A MAJ DON ENGEN THAYER HALL WEST POINT NY 10996-1786
1	DIRECTOR US ARMY RESEARCH LAB AMSRL CS AL TA 2800 POWDER MILL RD ADELPHI MD 20783-1145
3	DIRECTOR US ARMY RESEARCH LAB AMSRL CI LL 2800 POWDER MILL RD ADELPHI MD 20783-1145
	ABERDEEN PROVING GROUND
4	DIR USARL AMSRL CI LP (305)

NO. OF COPIES	ORGANIZATION
	ABERDEEN PROVING GROUND
65	DIR USARL AMSRL CI C NIETIBICZ C W STUREK AMSRL CI CB R KASTE (394) AMSRL CI S A MARK (309) AMSRL SL B AMSRL SL BA AMSRL SL BE D BELY AMSRL SL EI AMSRL WM B A HORST (390A) H ROGERS (120) E SCHMIDT (390A) AMSRL WM BA F BRANDON (120) W D'AMICO (120) C M SHOEMAKER (120) AMSRL WM BC P PLOSTINS (390) AMSRL WM BD B FORCH (390A) AMSRL WM BE T MINOR (390) AMSRL WM M D VIECHNICKI G HAGNAUR J MCCAULEY AMSRL WM MA R SHUFORD AMSRL WM MB B BURNS (4600) W DRYSDALE (4600) T BLANAS (4600) T BOGETTI R BOSSOLI (120) J BENDER (4600) L BURTON (4600) S CORNELISON (120) P DEHMER (4600) R DOOLEY (4600) B FINK G GAZONAS (4600) S GHIORSE (4600) D GRANVILLE (4600) D HOPKINS (4600)

NO. OF COPIES	ORGANIZATION
	C HOPPEL (4600) D HENRY (4600) R KASTE (4600) R KLINGER (4600) M LEADORE (4600) R LIEB (4600) F PIERCE (120) E RIGAS (4600) D SPAGNUOLO (4600) W SPURGEON (4600) J TZENG (4600) AMSRL WM MB(ALC) A ABRAHAMIAN M BERMAN A FRYDMAN T LI W MCINTOSH E A SZYMANSKI AMSRL WM MC R ADLER T HYNES J MONTGOMERY AMSRL WM MD W ROY AMSRL WM T W MORRISON (309) AMSRL WM TA W GILLICH (390) W BRUCHEY (390) AMSRL WM TC W DE ROSSET (309) R COATES (309) AMSRL WM TD T CHOU D DIETRICH (309) D PRITCHARD (4600)

REPORT DOCUMENTATION PAGE

Form Approved
OMB No. 0704-0188

1. AGENCY USE ONLY *(Leave blank)*	2. REPORT DATE	3. REPORT TYPE AND DATES COVERED
	September 1998	Final, June 1996 - September 1996

4. TITLE AND SUBTITLE

Structural Degradation of a Tank Cannon Due to Hole Damage

5. FUNDING NUMBERS

622618AH80

6. AUTHOR(S)

Larry Burton

7. PERFORMING ORGANIZATION NAME(S) AND ADDRESS(ES)

U.S. Army Research Laboratory
ATTN: AMSRL-WM-MB
Aberdeen Proving Ground, MD 21005-5069

8. PERFORMING ORGANIZATION REPORT NUMBER

ARL-TR-1796

9. SPONSORING/MONITORING AGENCY NAMES(S) AND ADDRESS(ES)

10.SPONSORING/MONITORING AGENCY REPORT NUMBER

11. SUPPLEMENTARY NOTES

12a. DISTRIBUTION/AVAILABILITY STATEMENT

Approved for public release; distribution is unlimited.

12b. DISTRIBUTION CODE

13. ABSTRACT ***(Maximum 200 words)***

An analysis was undertaken to determine the deleterious effects upon the M256 tank cannon's structural integrity if it were perforated. The analytical study looked at holes ranging in diameter from 1.5 in (3.8 cm) to 4.0 in (10 cm). Two perforation scenarios were modeled: one having a centered through hole and the other with a single hole centered on the cannon's wall. Finite element analysis runs were made to determine the extent of the plastic deformation that resulted from the introduction of the hole. Two locations along the barrel's length were considered: one near the muzzle end and the other at the tube's midsection. The muzzle end exhibited a greater depth of plastic stress with nearly one-third of the gun tube wall going into the plastic regime for the largest hole sizes.

14. SUBJECT TERMS

finite element, tank cannon, structural integrity, plastic deformation

15. NUMBER OF PAGES

24

16. PRICE CODE

17. SECURITY CLASSIFICATION OF REPORT	18. SECURITY CLASSIFICATION OF THIS PAGE	19. SECURITY CLASSIFICATION OF ABSTRACT	20. LIMITATION OF ABSTRACT
UNCLASSIFIED	UNCLASSIFIED	UNCLASSIFIED	UL

NSN 7540-01-280-5500

Standard Form 298 (Rev. 2-89)
Prescribed by ANSI Std. 239-18 298-102

INTENTIONALLY LEFT BLANK.

USER EVALUATION SHEET/CHANGE OF ADDRESS

This Laboratory undertakes a continuing effort to improve the quality of the reports it publishes. Your comments/answers to the items/questions below will aid us in our efforts.

1. ARL Report Number/Author ARL-TR-1796 (Burton) Date of Report September 1998
2. Date Report Received
3. Does this report satisfy a need? (Comment on purpose, related project, or other area of interest for which the report will be used.)
4. Specifically, how is the report being used? (Information source, design data, procedure, source of ideas, etc.)
5. Has the information in this report led to any quantitative savings as far as man-hours or dollars saved, operating costs avoided, or efficiencies achieved, etc? If so, please elaborate.
6. General Comments. What do you think should be changed to improve future reports? (Indicate changes to organization, technical content, format, etc.)

CURRENT ADDRESS

Organization

Name E-mail Name

Street or P.O. Box No.

City, State, Zip Code

7. If indicating a Change of Address or Address Correction, please provide the Current or Correct address above and the Old or Incorrect address below.

OLD ADDRESS

Organization

Name

Street or P.O. Box No.

City, State, Zip Code

(Remove this sheet, fold as indicated, tape closed, and mail.)

(DO NOT STAPLE)

DEPARTMENT OF THE ARMY

OFFICIAL BUSINESS

NO POSTAGE
NECESSARY
IF MAILED
IN THE
UNITED STATES

BUSINESS REPLY MAIL
FIRST CLASS PERMIT NO 0001,APG,MD

POSTAGE WILL BE PAID BY ADDRESSEE

DIRECTOR
US ARMY RESEARCH LABORATORY
ATTN AMSRL WM MB
ABERDEEN PROVING GROUND MD 21005-5069